

1 Modelled glacier equilibrium line altitudes during the mid- 2 Holocene in the southern mid-latitudes

3
4 **C. Bravo**^{1,2,3,*}, **M. Rojas**^{1,2,3}, **B. M. Anderson**⁴, **A. N. Mackintosh**⁴, **E. Sagredo**^{3,5}
5 **and P.I. Moreno**^{2,3,6}

6 [1]{Department of Geophysics, Universidad de Chile, Santiago, Chile}

7 [2]{Center for Climate and Resilience Research (CR2), Universidad de Chile, Santiago
8 Chile}

9 [3]{Millennium Nucleus Paleoclimate of the Southern Hemisphere, Santiago, Chile}

10 [4]{Antarctic Research Centre, Victoria University of Wellington, Wellington, New
11 Zealand}

12 [5] {Institute of Geography, Pontificia Universidad Católica de Chile, Santiago, Chile}

13 [6]{Department of Ecological Sciences and Institute of Ecology and Biodiversity,
14 Universidad de Chile, Santiago, Chile}

15 [*]{Now at Glaciology Laboratory, Centro de Estudios Científicos, Valdivia, Chile}

16 Correspondence to: Claudio Bravo (claudio@dgf.uchile.cl)

17 18 **Abstract**

19 Glacier behaviour during the Mid-Holocene (MH, 6000 year B.P.) in the Southern
20 Hemisphere provides observational data to constrain our understanding of the origin and
21 propagation of paleoclimate signals. In this study we examine the climatic forcing of
22 glacier response in the MH by evaluating modelled glacier equilibrium line altitudes
23 (ELAs) and climatic conditions during the MH compared with pre-industrial time (PI, year
24 1750). We focus on the middle latitudes of the Southern Hemisphere, specifically Patagonia
25 and the South Island of New Zealand. Climate conditions for the MH were obtained from
26 PMIP2 models simulations, which in turn were used to force a simple glacier mass balance
27 model to simulate changes in ELA. In Patagonia, the models simulate colder conditions
28 during the MH in the austral summer (-0.2°C), autumn (-0.5°C) and winter (-0.4), and

1 warmer temperatures (0.2°C) during spring. In the Southern Alps the models show colder
2 MH condition in autumn (-0.7°C) and winter (-0.4°C) warmer conditions in spring (0.3°C)
3 and no significant change in summer temperature.

4 Precipitation does not show significant changes, but exhibits a seasonal shift with less
5 precipitation from April to September and more precipitation from October to April during
6 the MH in both regions. The mass balance model simulates a climatic ELA that is 15 - 33 m
7 lower during the MH compared with PI conditions. We suggest that the main causes of this
8 difference are driven mainly by colder temperatures associated to the MH simulation.
9 Differences in temperature have a dual effect on glacier mass balance: (i) less energy is
10 available for melting during summer and early autumn and (ii) lower temperatures cause
11 more precipitation to fall as snow rather than rain in late autumn and winter, resulting in
12 more accumulation and higher surface albedo. For these reasons, we postulate that the
13 modelled ELA changes, although small, may help to explain larger glacier extents observed
14 by 6000 yr B.P. in South America and New Zealand.

15

16 **1 Introduction**

17 Deciphering the climate signals and glacial history of the mid-latitudes of the Southern
18 Hemisphere (Fig. 1) during the Holocene is key to unravelling the mechanism of climate
19 change that occurred during this period. During the last ~11500 years, a series of intervals
20 of rapid climate changes occurred worldwide (Mayewski et al., 2004). Reduction in
21 temperature and/or increases in precipitation during these periods have been recorded as
22 multiple glacial advances in different areas of the planet. Solomina et al. (2015) recently
23 provided a global review of Holocene glacier activity. Periods of renewed glacial activity,
24 known as Neoglaciations (Porter and Denton, 1967), were initially identified in the
25 Northern Hemisphere. However, during the last decades, numerous studies have shown
26 evidence of glacial advances, as well as climate variability during this period in the
27 Southern Hemisphere (approximately between 35° to 55° S). Most of these studies have
28 focused on Patagonia (e.g. Clapperton and Sugden, 1988; Porter, 2000; Rodbell et al., 2009;
29 Strelin et al., 2014) and in the Southern Alps in New Zealand (e.g. Gellatly et al., 1988;
30 Porter, 2000; Schaefer et al., 2009, Putnam et al. 2012, Kaplan et al. 2013).

1 In Patagonia (Fig. 1), a number of different Neoglacial chronologies have been produced
2 (e.g. Mercer, 1982; Aniya, 1995; Clapperton and Sugden, 1988; Aniya, 2013). However,
3 significant differences between these chronologies have not been fully resolved. The most
4 recent of these chronologies suggests that the largest advance in the Lago Argentino area
5 (50°S) occurred between 6000-5000 yr B.P. (Strelin et al., 2014).

6 In Southern Island of New Zealand (Fig. 1), on the other hand, notable periods of glacier
7 still stand or re-advance occurred during the early to mid-Holocene, as well as during the
8 last millennium (Schaefer et al. 2009, Putnam et al 2012). It appears that these centennial-
9 scale glacial events have been superimposed on a long-term trend of decreasing ice extent
10 that persisted for the entire Holocene (Schaefer et al. 2009, Putnam et al. 2012, Kaplan et
11 al. 2013).

12 In this context, it is clear that several aspects of the Neoglacial chronology of the southern
13 mid-latitudes (35°-55°S) are still inadequately understood, and more detailed chronologies
14 are needed. Particularly relevant for this study, is the lack of agreement regarding the
15 timing of the Neoglaciations in the southern mid-latitudes (Porter, 2000).

16 Understanding the climate and glacial history of the southern mid-latitudes is a prerequisite
17 for testing hypothesis regarding the origin and propagation of palaeoclimate signals, the
18 coupling of the ocean-atmosphere in the extra-tropics, and the interaction of low- and high-
19 latitude climate controls on hemispheric and global climate (Fletcher and Moreno, 2012,
20 Moreno et al., 2010, Rojas et al. 2009, Putnam et al. 2012). The mid-Holocene represents a
21 key moment in our late climate history. This period, within the current interglacial cycle
22 had important differences in orbital parameters with respect to the present conditions and
23 was devoid of influences from late-glacial climate change (Braconnot et al., 2007).
24 Although recent work has demonstrated that orbital forcing may not have played a critical
25 role in glacier behavior during cold phases of the last glacial cycle (Doughty et al., 2015),
26 the climatic boundary conditions at that time were very different than during the Holocene.
27 Considering the uncertainty in the timing of the beginning of the Neoglaciation, but that
28 geologic evidence suggest that glaciers were larger than present between 8000-6000 yr B.P.
29 in both regions (Kaplan et al., 2013, Schaefer et al., 2009, Putnam et al., 2012, Douglass et
30 al., 2005, Harrison et al., 2012), the aim of this work is to undertake a first-order modelling

1 study to assess if the climatic conditions during the mid-Holocene would permit the
2 existence of more extensive glaciers than during the Pre-Industrial (PI) period.

3 At the mid-Holocene (MH hereafter) orbital differences resulted in southern mid-latitudes
4 negative insolation anomalies from November through March and positive anomalies from
5 June to October in climate models (Rojas and Moreno, 2011). We expect that these
6 orbital/insolation differences had a major impact on the glacial extent and especially in the
7 equilibrium line altitudes (ELA) of glaciers. The equilibrium line altitude is a climatic
8 sensitive parameter marking the location on a glacier where accumulation of snow is
9 exactly balanced by ablation (net surface mass balance equals zero) (Porter 1975, Cogley et
10 al., 2011). ELA can be estimated by fitting a curve to data representing surface mass
11 balance as a function of altitude or a mass balance profile (Cogley et al., 2011). Also it is
12 possible to estimate a climatic ELA as an average of ELA during 30 or more years (Bakke
13 and Nesje, 2011). In this sense the most appropriate definition for a climatic ELA is the
14 steady-state ELA or long term ELA that could be estimated by modelling (Cogley et al.,
15 2011). Fluctuations of ELA have been extensively used in paleoclimatic reconstructions
16 because the ELA is primarily controlled by temperature and precipitation (Porter, 1975,
17 Sagredo et al., 2014).

18 In this paper, we explore the differences in the climatic ELA between the MH and the pre-
19 industrial (PI, hereafter) conditions, using a degree day model with data based on
20 Paleoclimate Modelling Intercomparison Project 2 (PMIP2) climate models output in the
21 Southern Alps in New Zealand and Patagonian Andes in South America (Fig. 1). Therefore
22 this study goes a further step towards linking PMIP2 model simulations, and hence orbital
23 forcing, with the MH glacial record, by explicitly calculating the regional ELAs in
24 Patagonia and New Zealand at 6000 yr B.P. The ELA difference between the PI and MH
25 provides information on the scale of glacier change at this key time.

26

27 **2 Data and methods**

28 **2.1 Experimental setup**

29 With the aim of obtaining comparable results we use a glacier mass balance model forced

1 with Paleoclimate Modelling Intercomparison Project 2 (PMIP2) models for both periods,
2 MH and PI. In the next sections we explain both, the model and the data. General approach
3 consists in resize all PMIP2 models output to a resolution of 0.5° using linear interpolation.
4 Due to the coarse resolution of the PMIP2 models, and the regional nature of this study, we
5 used the ELA as a general indicator of glacier behaviour as we are not considering
6 individual glaciers and their specific responses to climatic variations. For each grid point
7 we obtained surface mass balance as a function of altitude. From this mass balance profile
8 we obtained the ELA. Rather, we are interested in translating the output of the PMIP2
9 models into a signal that the glaciers respond to. Although the ELA is also determined by
10 local climate or topography factors, it is a good indicator of regional climate because
11 glacier mass-balance are commonly correlated over distances of 500 km (Bakke and Nesje,
12 2011) or even more distance. For example, in the Southern Alps of New Zealand today,
13 glacier end of summer snowlines (a proxy for the ELA) monitored by aerial survey
14 correlate over the ~800 km length of the Southern Alps (Chinn et al. 2005).

15 We applied the same procedure for both time slices (mid-Holocene and pre-Industrial) as
16 we are interested in a regional view of ELA change, hence we focus in the difference
17 between the two periods more than the absolute values of ELA, although we expect a
18 reasonable value for the ELA.

19 **2.2 Glacier Mass Balance Model**

20 We applied a simple glacier mass balance model to explore the regional differences in the
21 ELA between the MH and the PI in the southern mid-latitudes.

22 Although many of the ELA reconstructed are based in geologic evidence, ELA modelling
23 studies has been made. Degree-day models, as used in this study, have previously been
24 applied for palaeoclimate studies using data from general circulation models (GCM). As
25 examples, Hostetler and Clark (2000) used data from GENESIS (v. 2.01) simulations and
26 inferred ELA positions from mass balance profile curves for the LGM on tropical
27 glaciers. Rupper et al. (2009) also applied this kind of model to the region of Central
28 Asia, using data from re-analysis NCEP-NCAR for the present and data from general
29 circulation models of the phase I of PMIP for the Holocene. The aim was to reconcile
30 Holocene glacier history with climate by quantifying the change in ELA for simulated

1 changes in Holocene climate.

2 Details of the glacier mass balance model, which has been previously applied to Franz
3 Josef glacier, in New Zealand's Southern Alps, can be found in Anderson et al. (2006) and
4 are briefly described here. This model calculates the mass balance gradient for any specific
5 location, based on daily data of temperature and precipitation as a function of elevation.
6 Elevation in the model is defined for each grid point from 0 to 4000 m above sea level (asl)
7 with steps of 20 m. For each elevation, the mass balance is calculated based on:

$$8 \quad \dot{m}(t, z) = \dot{c}(t, z) + \dot{a}(t, z) \quad (1)$$

9 Where \dot{m} is the mass balance rate, \dot{c} the accumulation rate and \dot{a} the ablation rate at time t
10 and elevation z .

11 In glacier mass balance model, accumulation is defined as the portion of the daily
12 precipitation that falls as snow when the daily average temperature is below certain
13 temperature threshold (T_{crit}). Previous studies have considered T_{crit} being in the range of
14 0°C to 2°C (Radic and Hock, 2011). Therefore, water equivalent (w.e.) accumulation is
15 calculated based on the daily information of mean temperature (T_{mean}) and total daily
16 precipitation (p_d), and calculated as:

$$17 \quad c(t, z) = \delta_m p_d \begin{cases} \delta_m = 1, & T_{mean} < T_{crit} \\ \delta_m = 0, & T_{mean} \geq T_{crit} \end{cases} \quad (2)$$

18 In this case, T_{crit} was assumed as 1°C (Anderson et al., 2006).

19 In the middle-latitudes, the ablation process is mainly controlled by melting (Rupper and
20 Roe 2008). Temperature is a good predictor of melt because incoming longwave radiation
21 and turbulent heat fluxes are important terms in the energy balance that are closely related
22 to air temperature (Ohmura, 2001; Oerlemans, 2001). The other major component of the
23 energy balance, shortwave radiation, is also closely correlated to air temperature.

24 Ablation in the model is proportional to the mean daily temperature, and occurs for values
25 above 0°C (Braithwaite, 1985; Hock, 2005). In this study, we calculated ablation
26 using T_{mean} when this is positive:

$$27 \quad T_d^+(t, z) = \begin{cases} (T_{mean}(t, z) - 0), & T_{mean} > 0^\circ C \\ 0, & T_{mean} \leq 0^\circ C \end{cases} \quad (3)$$

1 Where T_d^+ is a positive daily temperature.
2 Ablation is calculated by multiplying the T_d^+ by a factor that relates temperature and
3 ablation, the degree day factor (DDF). The DDF (mm w.e. $d^{-1} C^{-1}$) corresponds to the
4 amount of melting (of ice and snow) per day, which occurs when temperatures are higher
5 than $0^\circ C$. This parameter shows great spatial variability and, in general, is higher for ice
6 and lower for snow due to the high albedo of the latter that reduces the absorption of
7 shortwave radiation (Braithwaite, 1995). In this study we use values of 6 and 3 mm w.e. d^{-1}
8 C^{-1} for ice and snow, respectively. These values correspond to the same values used by Woo
9 and Fitzharris (1992) for reconstructing the mass balance for Franz Josef glacier in the
10 Southern Alps. Therefore ablation is estimated by the following relationship:

$$11 \quad a(t, z) = DDF_{ice/snow} * T_d^+(t, z) \quad (4)$$

12 In this study, we use a DDF_{snow} when the snow depth is greater than zero, and DDF_{ice} when
13 the snow depth is equal to zero.

14 Note that, in this study, we assume that temperatures below zero do not contribute to
15 melting (Hock, 2003), and any potential contribution of sublimation to the total ablation is
16 neglected because it is likely small compared to melting.

17 By applying this model at different elevations, we obtain a glacier mass balance curve
18 (specific mass balance with altitude). The ELA occurs where the mass balance equals zero.
19 For the purpose of this study we assumed that some parameters such as temperature and
20 precipitation lapse rates, DDFs and temperature threshold T_{crit} , are constant and equal for
21 both the MH and the PI. Although this might not be strictly correct our focus here is on the
22 relative differences between the two periods rather than absolute values.

23 Given that the model has not previously been used in South America before, a preliminary
24 validation was carried out by comparing model results with existing glacier mass balance
25 data. Unfortunately, very few *in situ* glaciological mass balance measurements exist in
26 southern South America ($> 40^\circ S$). The most recent published mass balance study in this
27 area was at Mocho glacier, located on the Mocho-Choshuenco volcano ($39^\circ 55' S$,
28 $72^\circ 02' W$), which includes the hydrological year 2003/2004 (Rivera et al. 2005).

29 We assessed the performance of our model forced with climatological information coming

1 from a regional climate model at 25-km resolution and forced by the ERA40 reanalyses
2 (PRECIS-ERA40) in Mocho glacier in the Chilean Lake District (~40°S). Because the
3 ERA40 cover the period 1957-2001, we run the mass balance model for a 10 year period
4 (1980-1989) that does not correspond to the same year analysed in Rivera et al. (2005) with
5 the glaciological method (stakes). We hope that by running 10 years a climatological ELA
6 can be assessed. We use three precipitation lapse rates: 0, 0.00252 and 0.02 mm m⁻¹. This
7 comparison (not shown) showed a reasonable agreement between the observed and
8 modelled ELA, for the low precipitation lapse rates (0 and 0.00252 mm m⁻¹), with a
9 modelled ELA about 100 to 150 m below the observed, which is according to the glacier
10 recession documented for this glacier in the last 30 years (Rivera et al., 2005).

11

12 **2.3 Model inputs: PMIP2**

13 We use daily GCM temperature and precipitation values for computing the degree – day
14 model obtained from simulations carried out under the Paleoclimate Modelling
15 Intercomparison Project 2 (PMIP2), see Braconnot et al. (2007) for model setup and
16 boundary conditions.

17 Although PMIP is currently in its third phase (PMIP3) we used the modelling outputs of
18 PMIP2 given that daily data were not available for the most recent phase when this study
19 began. We analysed 7 models of the PMIP2 initiative (Table 1).

20 We compared the PI outputs with gridded temperature and precipitation data from CRU
21 TS3.10 and CRU TS3.10.01 (Harris et al., 2014) respectively and with weather station
22 observations to assess the climate model results (Supplement Figs. S1 to S4). The glacier
23 mass balance model was driven for 50 years to be able to capture the averaged influence
24 of inter-annual variability, with daily temperature and precipitation data derived from the
25 MH and PI experiments. With the purpose of comparing the ELA between the two
26 periods we calculated the mean mass balance for 50 years. Hence, the ELA calculated for
27 each period corresponds to a long-term or climatic ELA.

28 Temperature data were calculated for different elevations using a standard lapse rate of 6.5
29 °C km⁻¹. Due to the scarcity of available precipitation observations at high altitude,

1 especially in Patagonia (Garreaud et al., 2013), precipitation was corrected using a regional
2 mean observed gradient (in mm m^{-1}) in both regions. The observed gradient was obtained
3 using available latitudinal and altitudinal distributions of climate station data in both
4 regions. Fitting the precipitation versus altitude distribution yielded a mean value of
5 $0.00252 \text{ mm m}^{-1}$ in Patagonia and 0.0038 mm m^{-1} in New Zealand. Given that the
6 distribution of precipitation in mountainous regions is difficult to predict even under
7 present-day conditions (Rowan et al., 2014) we use this simple approach to facilitate the
8 process of mass balance modelling. In doing this, we are mindful that we are working at
9 mountain range scale, and that the PMIP2 models do not represent the precipitation
10 gradient very well, especially in the Southern Alps (Supplement Fig. S4). In addition a
11 constant precipitation factor (of 1.55) was also applied to account for the underestimation
12 that low resolution global models have of precipitation at high elevations (e.g. Rojas,
13 2006).

14 The results were averaged over 6 study zones. These zones correspond to: the Chilean Lake
15 District (CLD, approximately between 40° - 43° S), Northern Patagonian Icefield (NPI,
16 between 43° - 48° S), Southern Patagonian Icefield (SPI, between 48° - 53° S) and Cordillera
17 Darwin (CD, between 54° - 55° S) in South America, and the northern and southern sector of
18 the South Island of New Zealand (NZN, between 41.5° - 43.5° S; and NZS, 43.5° - 46° S,
19 respectively) (Fig. 1). Also we calculated climate differences between MH and PI over
20 these 6 zones using monthly PMIP2 data and tested their significance using a t –test in the
21 case of temperature, and a non-parametric Wilcoxon-Mann-Whitney test in the case of
22 precipitation with a significance level of 95 %.

23

24 **3 Results**

25 **3.1 Climate differences between the mid-Holocene and the pre-industrial**

26 Seasonal temperature differences between the MH and the PI (Fig. 2) are consistent
27 between most models, with temperature anomalies of the same sign and small inter-model
28 spread. Overall, in Patagonia, the models simulate colder conditions during the MH in the
29 austral summer (DJF), autumn (MAM) and winter (JJA), with average temperature
30 anomalies of $\sim -0.2^{\circ}\text{C}$, $\sim -0.5^{\circ}\text{C}$ and $\sim -0.4^{\circ}\text{C}$, respectively. During spring (SON) the PMIP2

1 models shows temperatures 0.2°C warmer.
2 In New Zealand (Fig. 2) the models show colder MH condition in austral autumn (~-0.7°C)
3 and winter (~-0.4°C), and warmer conditions in spring (~-0.3°C). In summer the intermodel
4 spread is larger, so that on average, the temperature anomalies are not significant. In the
5 annual mean, the temperature anomalies for South America and New Zealand are identical
6 (~-0.2°C). These temperature differences reflect the seasonal insolation difference between
7 the two periods. Estimates of precipitation change show less consistency than for
8 temperature (Fig. 3), and in several cases the models show precipitation anomalies of
9 different sign within regions. Nevertheless, there are some regions and seasons for which
10 the models show consistent precipitation changes. For example, during austral summer and
11 autumn the models suggest that the climate was wetter during the MH compared to PI, in
12 the CLD and the Patagonian Icefields. In general all zones exhibit drier winters than the PI;
13 spring was drier in the CLD and NPI, somewhat wetter in the SPI and CD and marginally
14 drier in the New Zealand zones. We find that the CLD was wetter in summer and autumn,
15 no change in winter and dryer in spring. Note that none of the precipitation changes are
16 statistically significant.

17 **3.2 ELA calculations and differences**

18 For ELA calculations, we excluded the FOAM model due to its unsatisfactory simulation of
19 the PI climate results (Supplement Figs. S1 to S4). The spatial distribution of the PI mean
20 ELA based on six PMIP2 models in Patagonia (Fig. 4), shows that the ELA values are
21 higher in the northern section of the study area, with maximum values above 2000 m asl
22 (mean value of 1800 m asl) in the CLD. To the south, the ELA decreases gradually,
23 reaching altitudes below 1000 m asl in SPI (mean value of 960 m asl) and CD (mean value
24 of 840 m asl, see Table 2). Our results also show that, in general, the inter-model variability
25 (one standard deviation) of the ELA estimation is small. One exception is the inter-model
26 variability observed in the SPI, where the maximum standard deviation is 250 m (mean
27 value of 140 m), in a region with mean ELA of about 950 m asl.

28 ELA estimates in New Zealand (Fig. 5) are higher in the northern part of South Island
29 (maximum values around 1800 m asl), and slowly decrease to values of 1400 m asl at the
30 southern tip of South Island (Table 2). These values show an approximate 200-400 m offset

1 (too high) in absolute terms, compared with observed values (e.g. Chinn et al., 2005). The
2 intermodel spread evaluated with the standard deviation is small in the northern part (148
3 m). South of 43°S, the intermodel spread becomes larger, with values between 150-180 m
4 on the western flank and up to 200 m on the eastern flank of the Southern Alps. The mean
5 value in this zone is 1530 m asl (Table 2).

6 As for the multi model mean ELA differences, in Patagonia (Fig. 6a) and in the Southern
7 Alps (Fig. 6) the ELA was lower during the MH compared to PI, however the magnitude of
8 change is relatively small: in Patagonia the mean difference is ~20 m in all zones, in the
9 Southern Alps is ~30 m in both zones. Besides the small estimated ELA variations, it is
10 important to highlight the consistency between ELA differences calculated by the PMIP2
11 models. In the Southern Alps, all of the six models indicate a negative sign in the ELA
12 differences between the MH and the PI (Fig. 6). In Patagonia at least four models show
13 negative differences between MH and the PI in almost the entire domain, with five models
14 showing a lower ELA during the MH in some parts of the CLD and SPI zones and six
15 models showing the same result in the west coast of the SPI zone (Fig. 6).

16

17 **4 Discussion**

18 **4.1 Difference between mid-Holocene and pre-industrial climates**

19 Rojas and Moreno (2011) evaluated the full PMIP2 MH simulations for the climatic
20 conditions in Patagonia and New Zealand. They found that both regions received less
21 precipitation during a colder accumulation season, and more precipitation during a warmer
22 ablation season. Therefore they suggested, on a qualitative basis, that the temperature and
23 precipitation anomalies could effectively lead to larger glacier during the MH and hence
24 explain Neoglaciation in both regions.

25 This paper goes a step further towards understanding the effects of climatic conditions on
26 glaciers and neoglaciations, and used those conditions to drive a glacier mass balance
27 model.

28 The differences in temperatures between the MH and the PI found in this study are similar
29 to those determined by Ackerley and Renwick (2010) for New Zealand, as well as Rojas

1 and Moreno (2011) for South America and New Zealand. Both studies analyzed data from
2 PMIP2 models, but used a different subset of models. Ackerley et al. (2013) use a regional
3 simulation of higher spatial resolution to simulate the MH climate, and also find a similar
4 temperature pattern found in this study. Given that all these studies indicate that the MH
5 was cooler than the PI in the autumn months and a warming in the spring months, we
6 conclude that the temperature signals are robust across different subset of PMIP2
7 simulations for the MH.

8 Our results indicate mostly wetter conditions during summer (DJF) and drier condition in
9 winter (JJA), in accordance with Rojas and Moreno (2011). For the autumn (MAM) and
10 spring (SON) seasons there is dipole-like signal, with positive precipitation anomalies in
11 the northern regions and drier conditions in the southern regions in MAM and the opposite
12 for SON. These results are also in fair accordance with Rojas and Moreno (2011). In the
13 New Zealand case, we find large inter-model spread between seasons, except during JJA
14 where we find a clear drier condition. Precipitation changes are slightly different than those
15 shown in Ackerley and Renwick (2010), which in turn do not agree with Rojas and Moreno
16 (2011) results. In summary, we found small changes in precipitation and large inter-modal
17 spread, so that existing studies discussed here give slightly different results.

18 **4.2 Differences between mid-Holocene and pre-industrial ELAs**

19 We observe that the mass balance model applied to Patagonia and New Zealand is able to
20 capture the expected differences in the climatological ELA associated with the climate
21 conditions estimated for the MH and the PI. Our results show that during the MH the ELA
22 could have been between 20-30 m lower than during the PI in Patagonia and New Zealand.

23 We propose that the results of the modelled ELA differences can be explained mainly by
24 the significant and consistent differences in modelled temperatures observed. The impact of
25 the precipitation anomalies are more difficult to assess, given that the climate data is
26 heterogeneous. This suggestion is consistent with the idea that glaciers from mid-latitudes
27 are more sensitive to changes in temperature than to changes in precipitation (Anderson and
28 Mackintosh, 2006). Moreover, we suggest that the observed differences in climatological
29 ELA are mainly driven by changes in the annual temperature cycle in these temperate
30 regions. In Patagonia, ablation dominantly occurs between September and March (spring

1 and summer months); whereas accumulation occurs from April to August (autumn and
2 winter months) (Rodbell et al., 2009). In New Zealand most of the ablation occurs between
3 November and April (summer and parts of spring and autumn), whereas accumulation
4 occurs from May to October (winter and parts of autumn and spring). However both
5 regions experience significant interannual variations, where accumulation or ablation
6 sometimes persists for longer period.

7 In Patagonia and New Zealand the lower summer temperatures observed during the MH
8 imply less energy input and hence lower amounts of melting. Although the opposite
9 happens in spring, where the higher temperatures of the MH indicate greater melting, we
10 suggest that this change was not sufficient to balance the impact of the lower summer
11 temperature on the mass balance. In addition, the lower temperatures observed during
12 autumn and winter would increase the percentage of precipitation falling as snow rather
13 than rain during the MH, as hypothetically suggested by Sagredo and Lowell (2012) and
14 Rodbell et al. (2009). This is particularly critical in the Southern Alps, where a significant
15 portion of the modern precipitation falls roughly at the elevation of the ELA. A temperature
16 drop in this area would result in an increment in snow precipitation (Rother and
17 Shulmeister, 2006). This can be particularly important in autumn and spring, when
18 temperatures in the vicinity of the ELA are typically -1 to 2 °C. Additionally precipitation
19 during winter is higher during the MH in almost all the PMIP2 models in all zones (Fig. 3),
20 this also contributes to accumulation and therefore a lower ELA in the MH with respect to
21 PI.

22 **4.3 ELA sensitivity to model parameters**

23 We performed sensitivity runs to increase the robustness of the modelling results in the
24 Patagonian and Southern Alps sectors. This motivated by the small differences in modelled
25 ELAs and the lack of constraints on important parameters owing to the scarcity of
26 measurements, especially in Patagonia. We investigated the sensitivity of ELA to the
27 precipitation lapse rate and the Degree Day Factor (DDF) of snow and ice.

28 We assessed precipitation lapse-rate values of 0, 0.001 and 0.02 mm m⁻¹ considering the
29 observed precipitation gradient in Patagonia and the Southern Alps of New Zealand
30 (0.00252 and 0.0038 mm m⁻¹ respectively). The sensitivity in the ELA difference to the

1 precipitation lapse rate has a maximum of 15 m in the northern part of Southern Island
2 (Fig.7) (glaciers do not exist in this zone). At the latitude of the northern glaciers of the
3 Southern Alps (approximately 43°S) the sensitivity is close to 10 m. Sensitivity declines
4 southward (see Fig. 7). In Patagonia (Fig. 8), the Chilean Lake District has a maximum
5 sensitivity of 6 m. This value is lower in the Northern Patagonia Icefield zone (2 to 3 m)
6 and close to 5 m in the Southern Patagonia Icefield. From both Figures it is clearer that in
7 almost all the study zone, for higher precipitation lapse rates values, the ELA differences
8 between the two periods become larger. We therefore conclude that the small ELA
9 differences in Patagonia and Southern Alps are significant and robust to this parameter and
10 therefore the results presented are the most conservative modelled ELA differences.

11 We assessed DDF values of 4, 8 and 10 mm d⁻¹ °C⁻¹ for ice and 2 and 4 mm d⁻¹ °C⁻¹ for
12 snow, within range of theoretical values used in the glacier modelling (3 mm d⁻¹ °C⁻¹ for
13 snow and 6 mm d⁻¹ °C⁻¹ for ice). DDF sensitivity is even lower in Southern Alps with a
14 maximum of 3 m in the northern part and also a reduction in the sensitivity to the south
15 (Fig. 7). In Patagonia sensitivity is 3 to 4 m along the Andes (Fig. 8).

16 **4.4 Comparison of geomorphically-reconstructed ELA and model results**

17 In the following paragraphs we assess our estimates of ELA change against some records of
18 neoglacial activity in both study areas

19 In Lago General Carrera (named Lago Buenos Aires in the Argentinean side, 46° 30' S),
20 central Patagonia, it has been shown that glaciers advanced around 6200 yr B.P. (Douglass
21 et al., 2005). Geomorphic evidence at this site suggests that during this glacial advance the
22 ELA dropped to 1100 m asl, a 300 m difference with respect to the present position
23 estimate for small isolated cirque glaciers. Further evidence of glacier activity is found by
24 Harrison et al. (2012) who determined ages of 5700 yr B.P. for a moraine located to the
25 west of the North Patagonian Icefield (46 ° 36 ' S / 73 ° 57 ' W) associated with San Rafael
26 glacier. Recently Strelin et al. (2014) found evidence for glacier advance between 6000 –
27 5000 yr B.P. based in moraine dating in the east side of Southern Patagonia Icefield (Lago
28 Argentino), specifically associated with the Upsala, Agassiz and Frías glaciers. However, in
29 the latter two studies, ELA differences were not calculated.

30 In the Southern Alps, geomorphic and geochronological evidence suggest that Tasman and

1 Mueller glaciers (43°50' S/170°E) advanced around 6740 ±160 yr B.P. (Schaefer et al.,
2 2009, age updated in Putnam et al., 2012). Putnam et al. (2012) demonstrated that a MH
3 glacial advance also occurred at Cameron glacier (~43°20'S/171°E) at 6890 ± 190 yr B.P.,
4 suggesting a regional event. In Putnam et al. (2012), ELA estimated for MH was ~140 m
5 lower than present, and 110 m lower than present 180±48 years ago. This suggests a fairly
6 modest change (~30 m) between the MH and PI, consistent with the results of the ELA
7 modelling in this work. While there is a systematic difference between the PI ELA
8 calculated by the model and modern observations, it is clear that relative changes in ELA
9 are very similar between our work and the estimates by Putnam et al. (2012).

10 The qualitative agreement in the direction of change between our modelling results and
11 geomorphic studies in these regions, despite absolute differences that are significantly
12 smaller (in the order of the tens of meters), lead us to conclude that the mass balance
13 modelling accounts for some but not all of the climatic differences between this two
14 periods.

15 Several caveats in our study account for more quantitative agreement in the absolute value
16 of the ELA. 1) We compare the MH simulations with PI conditions, which are different
17 from late 20th century climate. Reconstructions based on geologic evidence, on the other
18 hand, are compared against late 20th century conditions. 2) Glacier advances during the
19 mid-Holocene did not necessarily coincide with a precise time-slice, namely 6000 yr B.P.
20 3) The spatial scale of individual glaciers and the coarse resolution of climate models
21 hinder a direct comparison. 4) Important uncertainties are present in model parameters,
22 especially those related with the spatial distribution of precipitation and degree day factors.
23 5) The magnitude of the glacier expansion and mass balance from a given ELA change
24 depends on local conditions and characteristics of the glaciers, for example, glacier bed
25 slope and hypsometry (Oerlemans, 2012; De Angelis, 2014). Glacier bed slope is a primary
26 control on length sensitivity (Oerlemans, 2012) where a glacier with a gentle bed slope,
27 such as Upsala glacier in South Patagonia Icefield, shows a high length sensitivity to ELA
28 changes, estimated at ~-50 metres of glacier length per metre of ELA increase (Oerlemans,
29 2012). With this in mind we expected large change of the accumulation and ablation areas
30 even if the ELA oscillation is small (Mercer, 1965, Furbish and Andrews, 1984). In
31 contrast, the steep Franz Josef Glacier shows a much smaller length sensitivity of ~-10

1 metres of glacier length per metre of ELA increase. Glacier hypsometry is also an important
2 control on the sensitivity of mass balance to change in ELA, according to De Angelis
3 (2014) glaciers where the bulk of the area is located below the ELA are subject to the
4 largest changes of mass balance for any given changes in ELA. Considering all these
5 aspects and limitations of the glacier mass balance model, we highlight agreement among
6 both, the sign of change and regional homogeneity within and between both study regions.
7 This in-phase ELA response in Patagonia and New Zealand's South Island, is also in
8 agreement with glacier fluctuations observed during the 20th century where glaciers seem
9 to be in phase to similar climate forcing (Fitzharris et al., 2007).

10

11 **5 Conclusions**

12 A glacier mass balance model forced with PMIP2 simulations showed that southern mid-
13 latitude glacier ELAs during the mid-Holocene (MH) were lower compared to pre-
14 industrial (PI) conditions. The robustness of these results are evaluated by using six
15 different climate model data to run the mass balance model, as well as additional
16 simulations varying a number of not well constrained parameters of the model such as the
17 precipitation lapse-rate and the snow and ice degree day factors. The results of those
18 sensitivity simulations showed that the ELA differences, although small, had always the
19 same sign in New Zealand i.e., lower ELAs during the MH compared to PI and in most of
20 the models in Patagonia. We have therefore confidence that climatic conditions, as
21 simulated by six PIMIP2 models for MH conditions could lead to larger glaciers extents
22 during this period. The main forcing of the modelled ELA differences are temperature
23 differences. Significantly colder conditions during the summer, autumn and winter months
24 prevailed during the MH compared to the PI. In contrast, modelled precipitation changes
25 were small and with disagreement between models for the sign of change. Given that ELAs
26 for the MH were consistently lower despite the range of precipitation data they were forced,
27 our ELA results underline the evidence that temperate glaciers show a greater sensitivity to
28 temperature changes (Anderson and Mackintosh, 2006).

29 Temperature changes cause a double effect in glacier mass balance. First, in summer and
30 early autumn in the MH, less energy is available for melting and second, from autumn to

1 late winter, lower temperatures cause a larger portion of precipitation to fall as snow,
2 resulting in higher accumulation in the MH with respect to the PI, as well as a higher
3 surface albedo which reduces the amount of short-wave radiation available for melt.

4 This study provides new insights towards understanding southern hemisphere mid-
5 Holocene glacier conditions, demonstrating that orbital forcing inducing relatively coherent
6 temperature changes are consistent with a hemispheric pattern of larger glacier extent at
7 MH compared to the PI period

8

9 **Acknowledgments**

10 We acknowledge the international modelling groups for providing their data for analysis,
11 the Laboratoire des Sciences du Climat et de l'Environnement (LSCE) for collecting and
12 archiving the model data. The PMIP2/MOTIF Data Archive is supported by CEA, CNRS,
13 the EU project MOTIF (EVK2-CT-2002- 00153) and the Programme National d'Etude de
14 la Dynamique du Climat (PNEDC). This work is a contribution towards the SHAPE
15 (Southern Hemisphere Assessment of PalaeoEnvironments) project, which is supported by
16 the International Union for Quaternary Research. C. Bravo acknowledges the support of
17 CONICYT magister scholarship. The Millennium Nucleus NC120066 and CR2
18 N15110009 supported this investigation. M. Rojas and P.I. Moreno received support by
19 FONDECYT grant # 1131055. E. Sagredo acknowledges support by FONDECYT
20 Iniciación Grant # 11121280 and CONICYT Grant USA-2013-0035. A.N. Mackintosh and
21 B.M. Anderson acknowledge financial support from Victoria University Foundation Grant,
22 "Antarctic Research Centre Climate and Ice-Sheet Modelling". We would like to thank to
23 A.V. Rowan, one anonymous referee and J. Ubeda for their constructive and useful
24 comments.

25

26 **References**

27 Ackerley, D. and Renwick, A.: The Southern Hemisphere semiannual oscillation and
28 circulation variability during the Mid-Holocene, *Clim. Past*, 6, 415-430, 2010.
29 Ackerley, D., Lorrey, A., Renwick, J., Phipps, S., Wagner, S., and Fowler, A.: High

1 resolution modelling of mid-Holocene New Zealand climate at 6000 yr B.P., *Holocene*, 23,
2 1272-1285, 2013.

3 Anderson, B. and Mackintosh, A.: Temperature change is the major driver of late-glacial
4 and Holocene glacier fluctuations in New Zealand, *Geology*, 34, 121-124, 2006.

5 Anderson, B., Lawson, W., Owen, I., and Goodsell, B.: Past and future mass balance of
6 'KaRoimata o Hine Hukatere' Franz Josef Glacier, New Zealand, *J. Glaciol*, 52, 597-607,
7 2006.

8 Aniya, M.: Holocene glacial chronology in Patagonia: Tyndall and Upsala glaciers, *Arctic*
9 *Alpine Res.*, 27, 311-322, 1995.

10 Aniya, M.: Holocene glaciations of Hielo Patagónico (Patagonia Icefield), South America:
11 A brief review, *Geochemical Review*, 47, 97-105, 2013.

12 Bakke, J. and Nesje, A.: Equilibrium-Line Altitude (ELA), in: *Encyclopedia of Snow, Ice*
13 *and Glaciers*, edited by: Singh, V., Singh, P., and Haritashya, U., Springer, the Netherlands,
14 268– 277, 2011.

15 Braconnot, P., Otto-Bliesner, B., Harrison, S., Joussaume, S., Peterchmitt, J.-Y., Abe-Ouchi,
16 A., Crucifix, M., Driesschaert, E., Fichefet, Th., Hewitt, C. D., Kageyama, M., Kitoh, A.,
17 Lâiné, A., Loutre, M.-F., Marti, O., Merkel, U., Ramstein, G., Valdes, P., Weber, S. L., Yu,
18 Y., and Zhao, Y.: Results of PMIP2 coupled simulations of the Mid-Holocene and Last
19 Glacial Maximum - Part 1: experiments and large-scale features, *Clim. Past*, 3, 261-277,
20 doi:10.5194/cp-3-261-2007, 2007.

21 Braithwaite, R.: Calculation of degree-days for glacier-climate research, *Zeitschrift für*
22 *Gletscherkunde und Glazialgeologie* 20, 1-8, 1985.

23 Braithwaite, R.: Positive degree-day factors for ablation on the Greenland ice sheet studied
24 by energy-balance modelling, *J. Glaciol* 41, 153-160, 1995.

25 Chinn, T., Heydenrych, C., and Salinger, M.J.: Use of ELA as a practical method of
26 monitoring glacier response to climate in New Zealand's Southern Alps, *J. Glaciol*, 51, 85-
27 95, 2005.

28 Clapperton, C. and Sugden, D.: Holocene glacier fluctuations in South America and

- 1 Antarctica, *Quaternary Sci. Rev.*, 7, 185-198, 1988.
- 2 Cogley, J. G., Hock, R., Rasmussen, L. A., Arendt, A. A., Bauder, A., Braithwaite, R. J.,
3 Jansson, P., Kaser, G., Moller, M., Nicholson, L., and Zemp, M.: Glossary of Glacier Mass
4 Balance and Related Terms, IHP-VII Technical Documents in Hydrology No. 86, IACS
5 Contribution No. 2, UNESCO-IHP, Paris, 2011.
- 6 De Angelis, H.: Hypsometry and sensitivity of the mass balance to changes in equilibrium-
7 line altitude: the case of the Southern Patagonia Icefield, *Ann Glaciol*, 60, 14-28, 2014.
- 8 Douglass, D., Singer, B., Kaplan, M., Ackert, R., Mickelson, D., and Caffee, M.: Evidence
9 of early Holocene glacial advances in southern South America from cosmogenic surface-
10 exposure dating, *Geology* 33, 237-240, 2005.
- 11 Doughty, A., Scafefer, J., Putnam, A., Denton, G., Kaplan, M., Barrell, D., Andersen, B.,
12 Kelley, S., Finkel, R., and Schwartz, R.: Mismatch of glacier extent and summer insolation
13 in Southern Hemisphere mid-latitudes, *Geology*, 43, 407- 410, 2015.
- 14 Fitzharris, B., Clare, G., and Renwick, J.: Teleconnections between Andean and New
15 Zealand glaciers, *Global Planet. Change*, 59, 159-174, 2007.
- 16 Fletcher, M. and Moreno, P.: Have the Southern Weterlies changes in a zonally symmetric
17 manner over the last 14000 years? A hemisphere-wide take on a controversial problem,
18 *Quatern. Int.*, 254, 32-46, 2012.
- 19 Furbish, D. and Andrews, J.: The use of hypsometry to indicate long-term stability and
20 response of valley glaciers to changes in mass transfer, *J. Glaciol*, 30, 192-211, 1984.
- 21 Garreaud, R., Lopez, P., Minvielle, M., and Rojas, M.: Large Scale Control on the
22 Patagonia Climate, *J. Climate*, 26, 215-230, 2013.
- 23 Gellatly, A., Chinn, T. and Röthlisberger, F.: Holocene glacier variation in New Zealand: a
24 review, *Quaternary Sci. Rev.*, 7, 227-242, 1988.
- 25 Harris, I., Jones, P., Osborn, T., and Lister, D.: Updated high-resolution grids of monthly
26 climatic observations – the CRU TS3.10 Dataset, *Int. J. Climatol.*, 34, 623- 642, 2014.
- 27 Harrison, S., Glasser, N., Duller, G., and Jansson, K.: Early and mid-Holocene age for the
28 Tempanos moraine, Laguna San Rafael, Patagonian Chile, *Quaternary Sci. Rev.*, 31, 82- 92,

1 2012.

2 Hock, R.: Temperature index melt modelling in mountains areas, *J. Hydrol.*, 282, 104-115,
3 2003.

4 Hock, R.: Glacier melt: a review of processes and their modelling, *Prog. Phys. Geog.*, 29,
5 362-391, 2005.

6 Hostetler, S., and Clark, P.: Tropical climate at the Last Glacial Maximum inferred from
7 glacier mass-balance modelling, *Science*, 290, 1747-1750, 2000.

8 Kaplan, M., Schaefer, J., Denton, G., Doughty, A., Barrel, D., Chinn, T., Putnam, A.,
9 Andersen, B., Mackintosh, A., Finkel, R., Schwartz, R., and Anderson, B.: The anatomy of
10 long-term warming since 15 ka in New Zealand based on net glacier snowline rise,
11 *Geology*, 41, 887-890, doi:10.1130/g34288.1, 2013.

12 Mayewski, P., Rohling, E., Stager, J., Karlén, W., Maasch, K., Meeker, L., Meyerson, E.,
13 Gasse, F., Van Kreveld, S., Holmgren, K., Lee-Thorp, J., Rosqvist, G., Rack, F.,
14 Staubwasser, M., Schneider, R., and Steig, E.: Holocene climate variability, *Quaternary*
15 *Res.*, 62, 243 -255, 2004.

16 Mercer, J.: Glacier variations in southern Patagonia, *Geogr. Rev.*, 55, 390- 413, 1965.

17 Mercer, J.: Holocene glacier variation in southern South America, *Striae*, 18, 35-40, 1982.

18 Moreno P., Francois, J.P., Villa-Martinez, R., and Moy, C.: Covariability of the Southern
19 Westerlies and atmospheric CO₂ during the Holocene, *Geology*, 38, 727-730, 2010.

20 Oerlemans, J.: *Glaciers and climate change*. A.A. Balkema Publisher, Lisse, 2001.

21 Oerlemans, J.: Linear modelling of glacier length fluctuations, *Geogr. Ann. A.*, 94, 183-194.
22 doi: 10.1111/j.1468-0459.2012.00469.x, 2012.

23 Ohmura, A.: Physical basis for the Temperature-Based Melt-Index Method, *J. Appl.*
24 *Meteorol.*, 40, 753-761, 2001.

25 Porter, S.: Onset of Neoglaciation in Southern Hemisphere, *J. Quaternary Sci.*, 15, 395-
26 408, 2000.

27 Porter, S. and Denton, G.: Chronology of Neoglaciation in the North American Cordillera,

- 1 Am. J. Sci., 265, 177- 210, 1967.
- 2 Porter, S.: Equilibrium line altitudes of late Quaternary glaciers in the Southern Alps, New
3 Zealand, Quaternary Res., 5, 27-47, 1975.
- 4 Putnam, A., Schaefer, J., Denton, G., Barrel, D., Finkel, R., Anderson, B., Schwartz, R.,
5 Chinn, T., and Doughty, A.: Regional climate control of glaciers in New Zealand and
6 Europe during the pre-industrial Holocene, Nat. Geosci. 5, 627-630,
7 Doi:10.1038/ngeo1548, 2012.
- 8 Radic, V. and Hock, R.: Regionally differentiated contribution of mountain glaciers and ice
9 caps to future sea level rise, Nat. Geosci.s, 4, 91- 94, 2011.
- 10 Rivera, A., Bown, F., Casassa, G., Acuña, C., and Clavero, J.: Glacier shrinkage and
11 negative mass balance in the Chilean Lake District (40°S). Hydrolog Sci J 50, 963- 974,
12 2005.
- 13 Rodbell, D., Smith, J., and Mark. B.: Glaciation in the Andes during Lateglacial and
14 Holocene, Quaternary Sci. Rev., 28, 2165-2212, 2009.
- 15 Rojas, M.: Multiple Nested Regional Climate Simulations for Southern South America:
16 Sensitivity to Model Resolution. Mon. Weather Rev., 134, 2208-2223, 2006.
- 17 Rojas, M., Moreno, P., Kageyama, M., Crucifix, M., Hewitt, C., Abe, A., Ohgaito, R.,
18 Brady, E., and Hope, P.: The Last Glacial Maximum in the Southern Hemisphere in PMIP2
19 simulations. Clim. Dynam., 32, 525-548, 2009.
- 20 Rojas, M. and Moreno, P.: Atmospheric circulation changes and neoglacial conditions in
21 the Southern Hemisphere mid-latitudes: insights from PMIP2 simulation at 6 kyr, Clim.
22 Dynam., 37, 357- 375, 2011.
- 23 Rother, H. and Shulmeister, J.: Synoptic climate change as a driver of late Quaternary
24 glaciations in the mid-latitudes of the Southern Hemisphere. Clim. Past, 2, 11-19, 2006.
- 25 Rowan, A., Brocklehurst, S., Schultz, D., Plummer, M., Anderson, L. And Glasser, N.: Late
26 Quaternary glacier sensitivity to temperature and precipitation distribution in the Southern
27 Alps of New Zealand, J Geophys Res Earth Surf, 119, 1064-1081, 2014.
- 28 Rupper, S. and Roe, G.: Glacier change and regional climate: A mass and energy balance

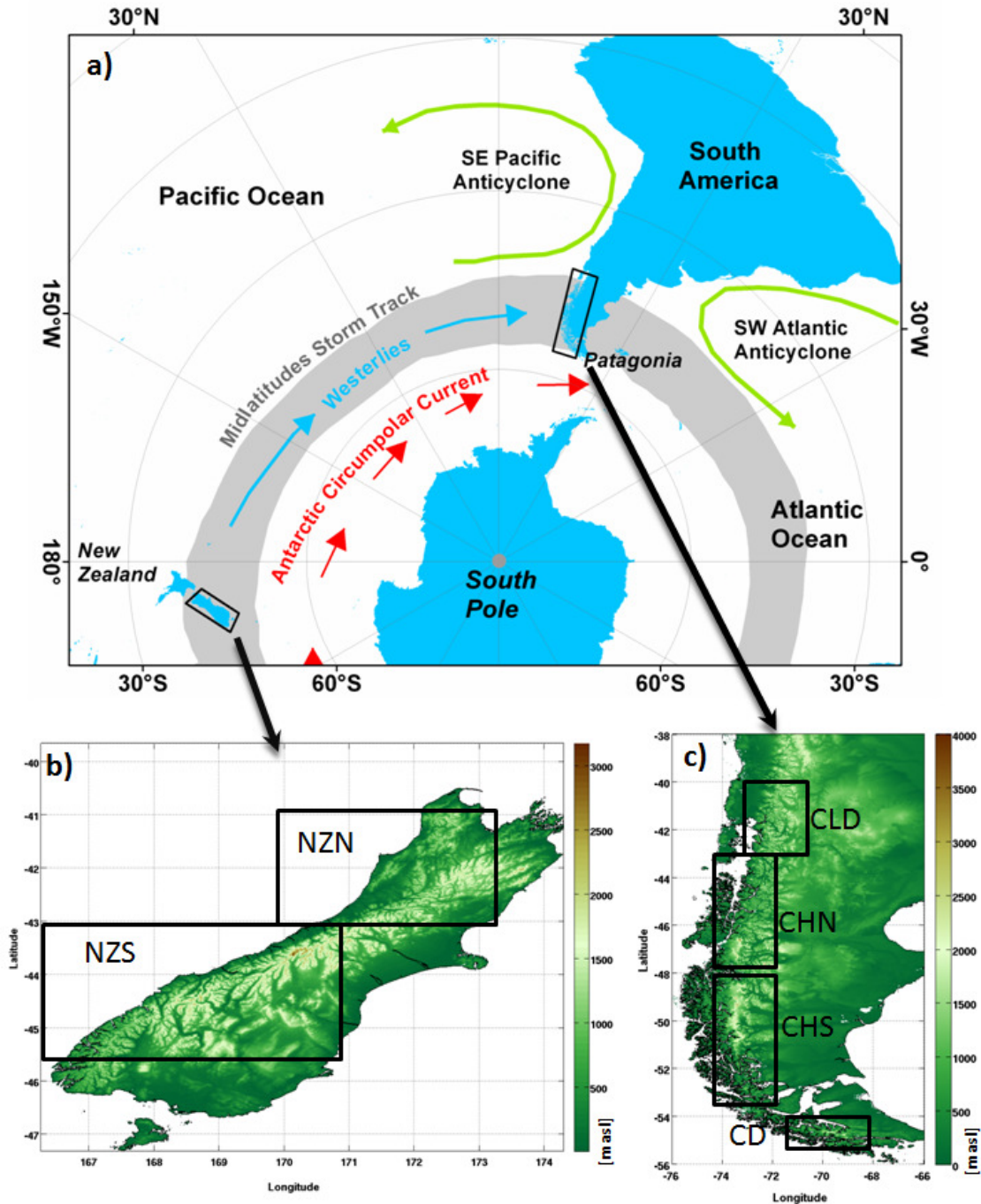
- 1 approach, *J. Climate*, 21, 5384-5401, 2008
- 2 Rupper, S., Roe, G., and Gillespie, A.: Spatial patterns of Holocene glacier advance and
3 retreat in Central Asia, *Quaternary Res.*, 72, 337- 346, 2009.
- 4 Sagredo, E. and Lowell, T.: Climatology of Andean glaciers: A framework to understand
5 glacier response to climate change, *Global Planet. Change*, 86-87, 101-109, 2012.
- 6 Sagredo, E., Rupper, S., and T. Lowell, T.: Sensitivities of the equilibrium line altitude to
7 temperature and precipitation changes along the Andes, *Quaternary Res.*, 81, 355-366,
8 2014.
- 9 Schaefer, J., Denton, G., Kaplan, M., Putman, A., Finkel, R., Barrel, D., Anderson, B.,
10 Schwartz, R., Mackintosh, A., Chinn, T., and Schluchter, C.: High-frequency Holocene
11 glacier fluctuation in New Zealand differs from the Northern signature, *Science*, 324, 622-
12 625, 2009.
- 13 Solomina, O., Bradley, R., Hodgson, D.A., Ivy-Ochs, S., Jomelli, V., Mackintosh, A.,
14 Nesje, A., Owen, L., Wanner, H., Wiles, G.C., and Young, N.E.: Holocene glacier
15 fluctuations. *Quaternary Sci. Rev.*, 111,9-34, 2015.
- 16 Strelin,J., Kaplan, M., Vandergoes, M., and Denton, G.: Holocene glacier history of the
17 Lago Argentino basin, Southern Patagonian Icefield, *Quaternary Sci. Rev.*, 101, 124-145,
18 2014.
- 19 Woo, M and B. Fitzharris, B.: Reconstruction of mass balance variations for Franz Josef
20 Glacier, New Zealand, 1913-1989, *Arctic Alpine Res.*, 24 (4), 281-290, 1992.

1 Table 1. PMIP2 models used in this study.

Models	Atmosphere lon x lat	Vertical levels	Years of data used
CSIRO-Mk3L-1.1	5.625 x ~ 3.18	18	50
ECHAM5-MPIOM1	3.75 x 2.5	20	50
FOAM	7.5 x 4.5	18	50
MIROC3.2	2.8 x 2.8	20	50
MRI-CGCM2.3.4fa	2.8 x 2.8	30	50
MRI-CGCM2.3.4nfa	2.8 x 2.8	30	50
UBRIS-HadCM3M2	3.75 x 2.5	19	50

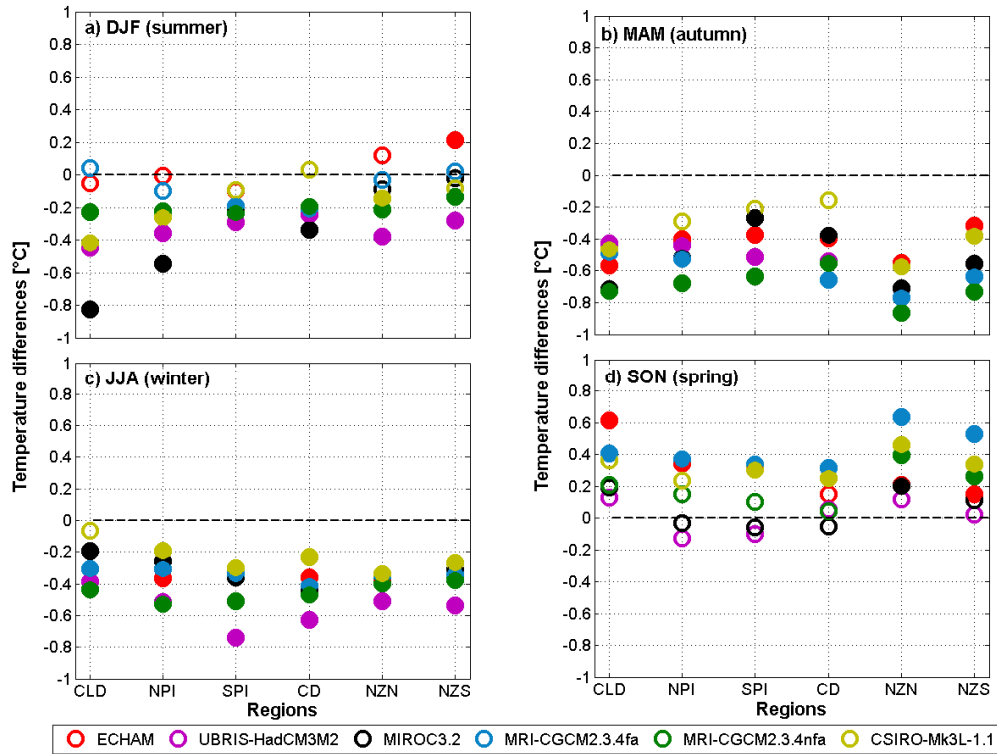
1 Table 2. Mean values of ELA for each zone

Region	Zones	ELA MH [m asl]	ELA PI [m asl]	Difference [m]
Patagonia	Chilean Lake District	1776 ± 99	1797 ± 93	-21±6
	Northern Patagonia			
	Icefield	1333 ± 125	1354 ± 106	-21±3
	Southern Patagonia			
	Icefield	939 ± 148	956 ± 140	-17±5
	Cordillera Darwin	821 ± 90	839 ± 89	-18±4
South Island,	North	1667 ± 144	1697 ± 148	-30±10
New Zealand	South	1501 ± 176	1528 ± 176	-27±6



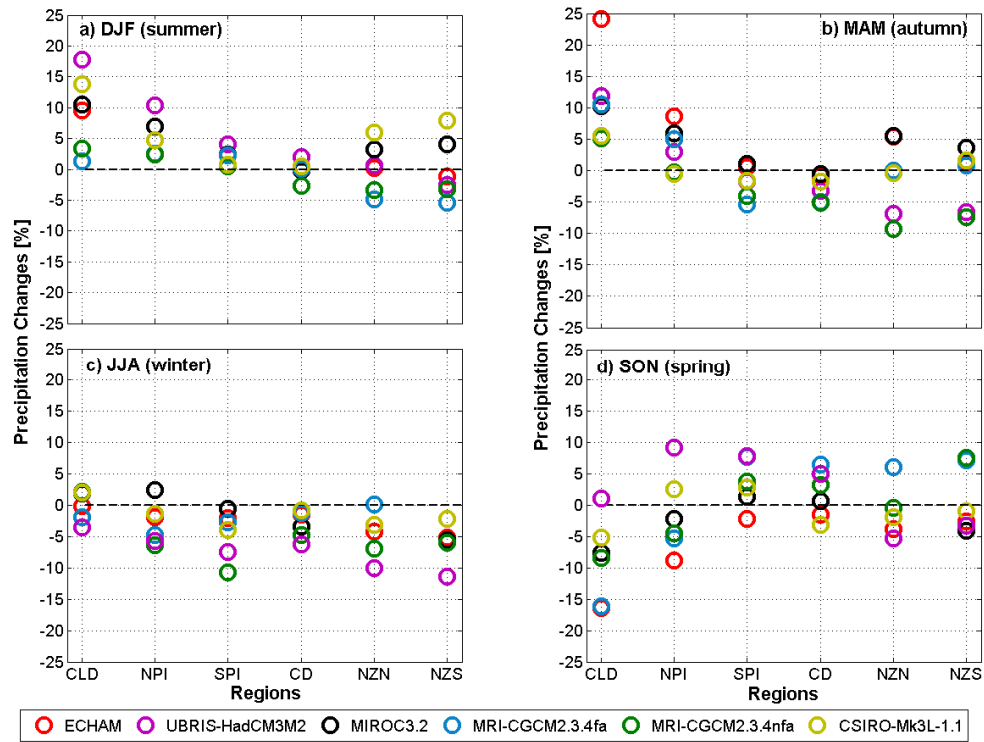
1

2 Figure 1. Study area. (a) Schematic diagram showing some of the main climate
 3 characteristics in the southern mid-latitudes. (b) New Zealand southern island topography
 4 and the two zones of analysis (NZN: New Zealand north, NZS, and New Zealand south).
 5 (c) Patagonia topography and the four zones of analysis (CLD: Chilean Lake District,
 6 CHN: North Patagonian Icefield, CHS: South Patagonian Icefield and CD: Cordillera
 7 Darwin).



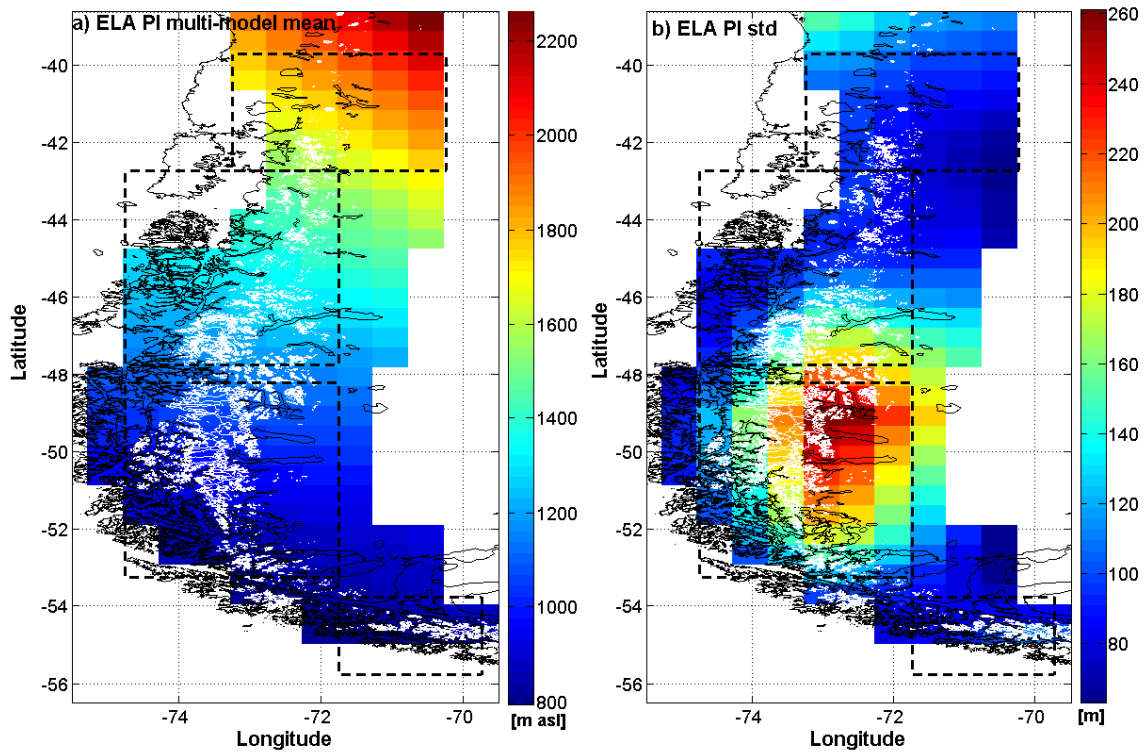
1

2 Figure 2. Temperature differences: Mid-Holocene minus Preindustrial, over the 6 zones of
 3 analysis. (a) DJF, (b) MAM, (c) JJA, (d) SON. Filled circles correspond to statistically
 4 significant differences ($p \leq 0.05$).



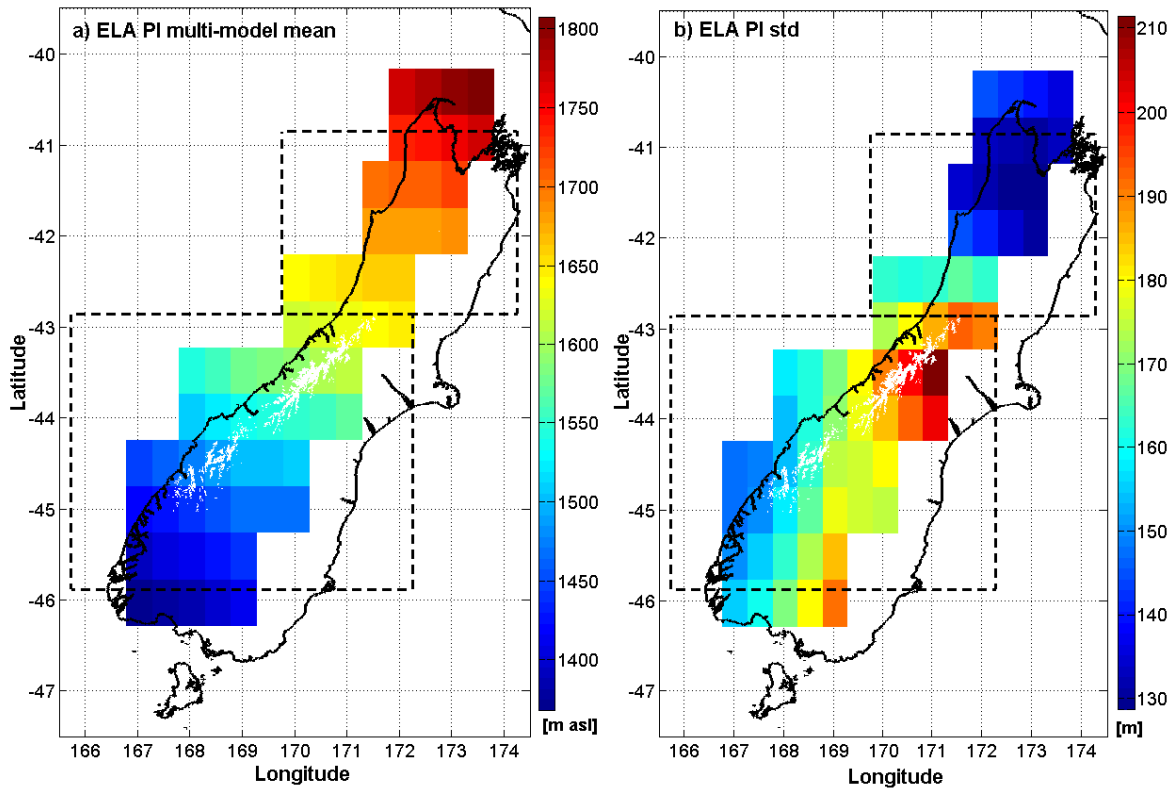
1

2 Figure 3. Precipitation differences: Mid-Holocene minus Preindustrial, over the 6 zones of
 3 analysis. (a) DJF, (b) MAM, (c) JJA, (d) SON. Filled circles correspond to statistically
 4 significant differences ($p \leq 0.05$).



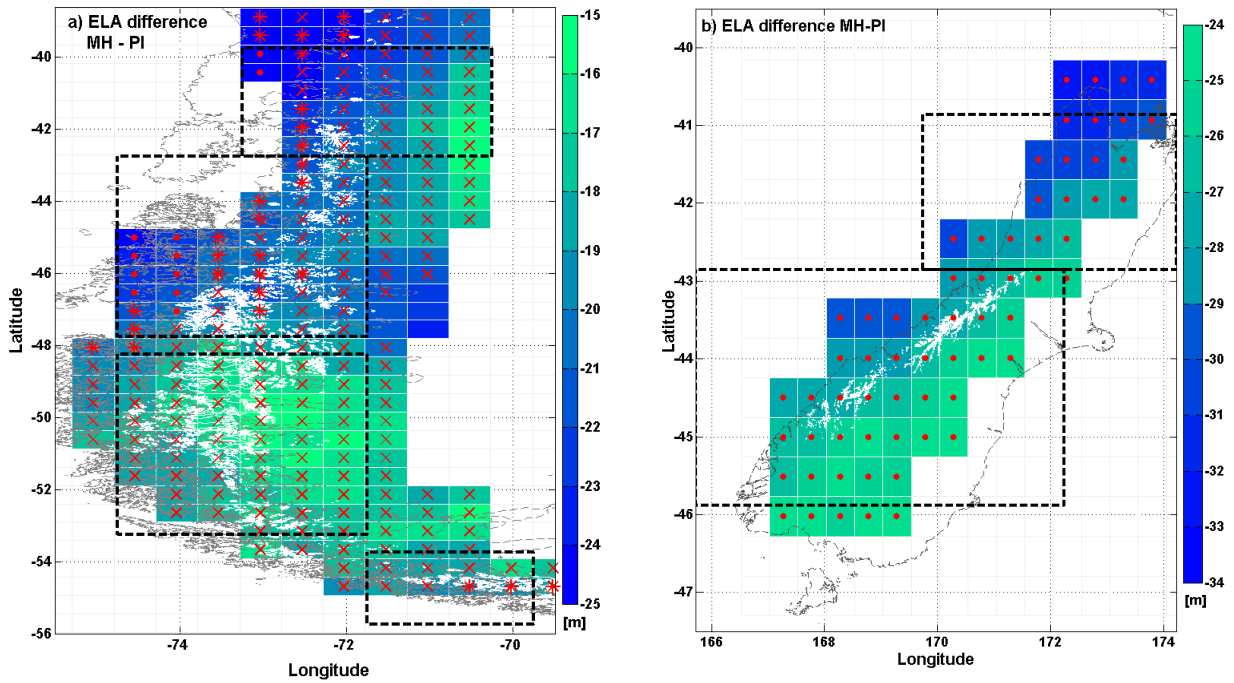
1

2 Figure 4. Spatial distribution of pre-industrial equilibrium line altitude (ELA) in South
 3 America based on six PMIP2 simulations. (a) mean ELA (m asl) and (b) inter-model
 4 variability of the ELA (one standard deviation). White lines correspond to actual glacier
 5 extension according to the Randolph Glacier Inventory (RGI 3.2)



1

2 Figure 5. Spatial distribution of pre-industrial equilibrium line altitude (ELA) in Southern
 3 Island of New Zealand based on six PMIP2 simulations. (a) Mean ELA (m asl) and (b)
 4 inter-model variability of the ELA (one standard deviation). White lines correspond to
 5 actual glacier extension according to the Randolph Glacier Inventory (RGI 3.2)

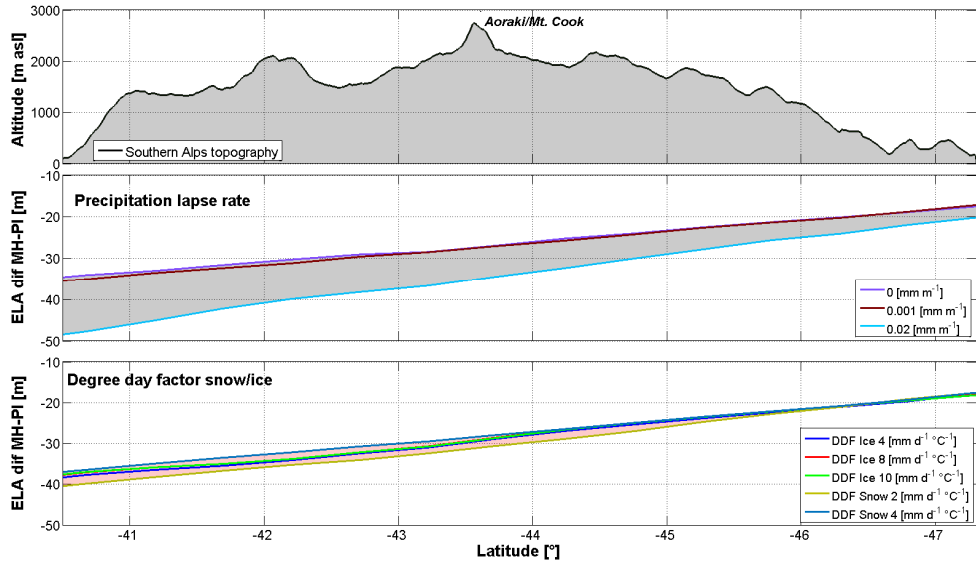


1

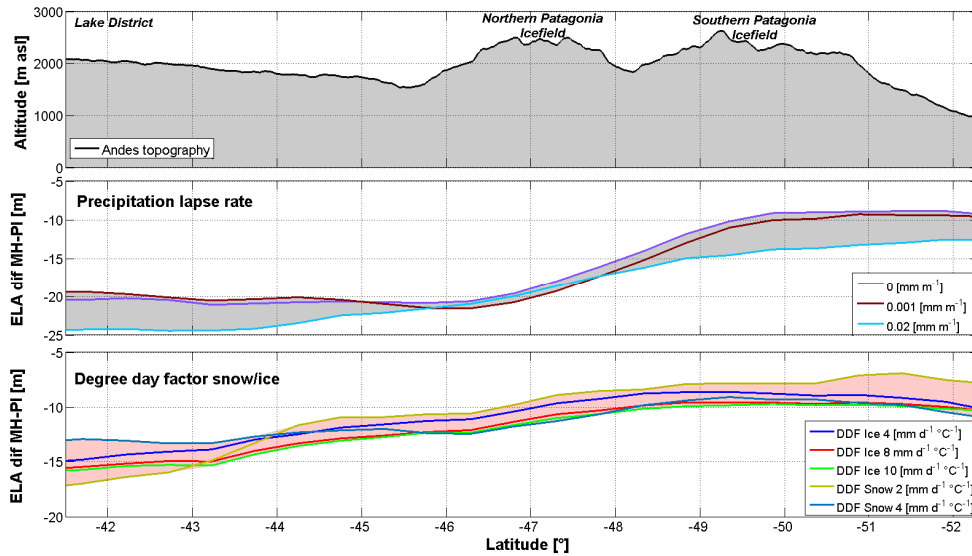
2 Figure 6. Mid-Holocene minus pre-industrial equilibrium line altitude differences. Points
 3 indicate that the six models have a negative sign in the differences; asterisks indicate that
 4 five models have a negative sign and crosses indicate that four models have a negative sign.
 5 White lines indicate actual glacier outlines (Randolph Glacier Inventory 3.2). a) Patagonia,
 6 b) New Zealand.

7

8



1
 2 Figure 7. Sensitivity of ELA differences in Southern Alps to precipitation lapse rate and
 3 degree day factor of snow and ice. a) Latitudinal topography profile of Patagonia (SRTM 1
 4 km) b) ELA difference sensitivity to precipitation lapse rate and c) ELA difference
 5 sensitivity to degree day factor of snow and ice. Gray and pink areas in b) and c) represent
 6 the range in ELA differences between MH and PI.



1

2 Figure 8. Sensitivity of ELA differences in Patagonian Andes to precipitation lapse rate and
 3 degree day factor of snow and ice. a) Latitudinal topography profile of Patagonia (SRTM 1
 4 km) b) ELA differences sensitivity to precipitation lapse rate and c) ELA differences
 5 sensitivity to degree day factor of snow and ice. Gray and pink areas in b) and c) represent
 6 the range in ELA differences between MH and PI.

7

8

9

10